

Fine-Tuning of Photophysical and Electronic Properties of Materials for Photonic Devices Through Remote Functionalization

Andreas M. Bünzli,^[a] Henk J. Bolink,^[b,c] Edwin C. Constable,^{*,[a]} Catherine E. Housecroft,^{*,[a]} Markus Neuburger,^[a] Enrique Ortí,^[b] Antonio Pertegás,^[b] and Jennifer A. Zampese^[a]

Keywords: Iridium / Ligand design / Photophysical properties / Electroluminescence / X-ray diffraction

We report four new iridium(III) complexes of the type $[\text{Ir}(\text{ppy})_2(\text{N}^{\wedge}\text{N})][\text{PF}_6]$ in which $\text{N}^{\wedge}\text{N}$ is a 4,6-diphenyl-2,2'-bipyridine and the 4-phenyl ring is substituted at either the *para* or *meta* positions [4-Me, $\text{N}^{\wedge}\text{N} = \mathbf{1}$; 4-Br, $\text{N}^{\wedge}\text{N} = \mathbf{2}$; 3,5-Br₂, $\text{N}^{\wedge}\text{N} = \mathbf{3}$; 3,5-(C₆H₄-4-NPh₂)₂, $\text{N}^{\wedge}\text{N} = \mathbf{4}$]. The complexes have been fully characterized, and single-crystal diffraction analyses of $[\text{Ir}(\text{ppy})_2(\text{N}^{\wedge}\text{N})][\text{PF}_6]$ ($\text{N}^{\wedge}\text{N} = \mathbf{1-3}$) confirmed that each $[\text{Ir}(\text{ppy})_2(\text{N}^{\wedge}\text{N})]^+$ cation exhibits face-to-face π -stacking between the pendant phenyl substituent of the $\text{N}^{\wedge}\text{N}$ ligand and the cyclometallated phenyl ring of an adjacent $[\text{ppy}]^-$ ligand. In solution, the complexes are short-lived emitters; the emission maxima for $[\text{Ir}(\text{ppy})_2(\mathbf{1})][\text{PF}_6]$, $[\text{Ir}(\text{ppy})_2(\mathbf{2})][\text{PF}_6]$, and

$[\text{Ir}(\text{ppy})_2(\mathbf{4})][\text{PF}_6]$ are similar ($\lambda_{\text{em}} = 600\text{--}608\text{ nm}$), but the presence of the two bromo substituents in $[\text{Ir}(\text{ppy})_2(\mathbf{3})][\text{PF}_6]$ produces a redshift of ca. 30 nm. The solid-state photoluminescent emission spectra of thin films of the complexes are similar to those in solution. The performances of the complexes as electroluminescent components in light-emitting electrochemical cells (LECs) have been evaluated. The electroluminescence spectra show slight blueshifts with respect to the photoluminescence bands. LEC turn-on times vary from instantaneous for $\text{N}^{\wedge}\text{N} = \mathbf{2}$ to 2 h for $\text{N}^{\wedge}\text{N} = \mathbf{1}$. The device data suggest that the incorporation of Br substituents into the $\text{N}^{\wedge}\text{N}$ co-ligand may not be beneficial.

Introduction

Octahedral iridium(III) complexes of the type $[\text{Ir}(\text{ppy})_2\text{L}]^+$, in which $[\text{ppy}]^-$ is the cyclometallated 2-phenylpyridinato ligand and L is a neutral, bidentate ligand, are currently being developed for application in light-emitting electrochemical cells (LECs).^[1] These devices incorporate ionic, heavy d-block metal complexes in the light-emitting layer. Efficient electroluminescence can be achieved by using salts of $[\text{Ir}(\text{ppy})_2\text{L}]^+$ in which L is an $\text{N}^{\wedge}\text{N}$ chelating ligand. The first breakthrough came with the efficient performance of $[\text{Ir}(\text{ppy})_2(\text{dtbbpy})][\text{PF}_6]$ (dtbbpy = 4,4'-di-*tert*-butyl-2,2'-bipyridine).^[2] Since this report, much progress has been made through combined experimental and theoretical studies to effectively tune the electroluminescent behaviour of this family of emitters^[3-5] and by combining orange and blue emitters to produce white light-emitting LECs.^[6-9] Tuning the emission wavelength is achieved by functionalizing the $[\text{ppy}]^-$ ligands and/or varying and functionalizing the $\text{N}^{\wedge}\text{N}$

ligand,^[10,11] and a combinatorial approach has been used for rapid screening of potential emitters.^[12] An inherent problem of the iridium(III) emitters is their limited stability in LEC devices.^[13,14] To overcome this we are currently focusing on a strategy to exploit intracation face-to-face π -stacking between $[\text{ppy}]^-$ and $\text{N}^{\wedge}\text{N}$ chelating ligands to increase device lifetimes,^[15-20] a strategy previously shown to have profound effects on the photophysical properties of this class of compounds.^[21] The success of this approach has led us to screen many $[\text{Ir}(\text{ppy})_2(\text{N}^{\wedge}\text{N})]^+$ complexes to gain a better appreciation of the structural and electronic properties of the ligand that result in improved performances in LECs. Our approach has been to explore the structures in the complexes to independently optimize the cyclometallation and N,N' -donor ligands in conjunction with computational studies to ensure the desired colour is achieved.

In this paper we describe four complexes of the type $[\text{Ir}(\text{ppy})_2(\text{N}^{\wedge}\text{N})][\text{PF}_6]$. The ligand $\text{N}^{\wedge}\text{N}$ is based on 4,6-diphenyl-2,2'-bipyridine in which the 4-phenyl ring is substituted at either the *para* or *meta* positions (Scheme 1). The 6-phenyl substituent is included in the ligand design to facilitate the intracation π -stacking. The *para*-substituted ligands **1** and **2** contain electron-releasing and -withdrawing substituents, respectively, and on going from **2** to **3**, the electron-withdrawing effects are enhanced. The bromo derivatives **2** and **3** are useful building blocks for further functionalization, and this is exemplified by the conversion of **3** into

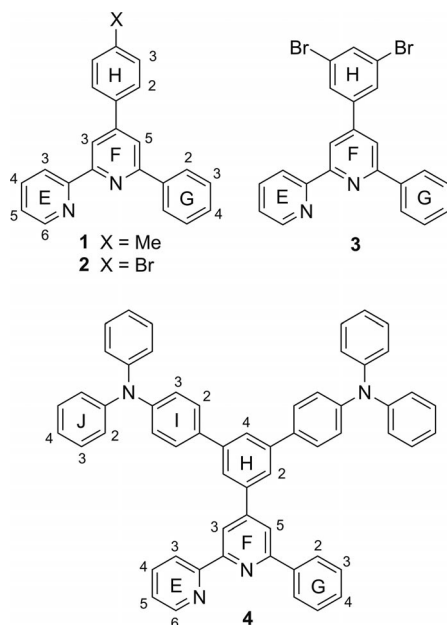
[a] Department of Chemistry, University of Basel, Spitalstrasse 51, 4056 Basel, Switzerland
Fax: +41-61-267-1008
E-mail: edwin.constable@unibas.ch
catherine.housecroft@unibas.ch

[b] Instituto de Ciencia Molecular, Universidad de Valencia, Catedrático José Beltrán 2, 46980 Paterna, Spain

[c] Fundació General de la Universidad de Valencia (FGUV), P. O. Box 22085, 46010 Valencia, Spain

Supporting information for this article is available on the WWW under <http://dx.doi.org/10.1002/ejic.201200394>.

4, which contains electron-donating triphenylamino substituents. Although the complex $[\text{Ir}(\text{ppy})_2(\mathbf{1})][\text{PF}_6]$ has been previously reported,^[19] it has not, to the best of our knowledge, been tested in LEC devices. The aim of this study was to compare the solution and solid-state properties of $[\text{Ir}(\text{ppy})_2(\text{N}^{\wedge}\text{N})][\text{PF}_6]$ with $\text{N}^{\wedge}\text{N} = \mathbf{1-4}$, including their performances in LEC devices.



Scheme 1. Structures of ligands **1-4** and atom labelling for NMR spectroscopic assignments.

Results and Discussion

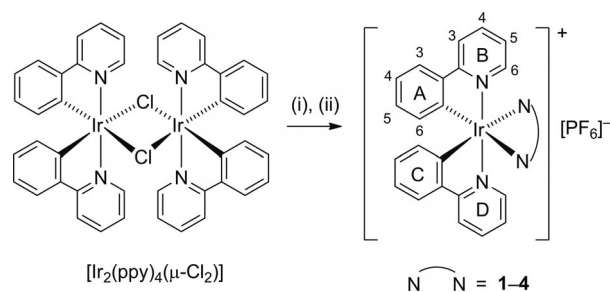
Ligand Synthesis and Characterization

Compound **1** has previously been reported,^[19,22] but we chose to prepare the ligand by using the solventless, grinding method of Cave and Raston.^[23] Compounds **1**, **2** and **3** were prepared by sequential aldol condensation of acetophenone and 4-methylbenzaldehyde, 4-bromobenzaldehyde or 3,5-dibromobenzaldehyde, respectively, in the presence of base, followed by Michael addition of 2-acetylpyridine, and finally addition of ammonium acetate. After column chromatography, **1-3** were isolated in yields of 19–26%. Compound **4** was prepared by palladium-catalysed Suzuki coupling of **3** with 4-(diphenylamino)phenylboronic acid and was isolated in 82% yield. For **1**, the ¹H NMR spectroscopic data are consistent with those previously published,^[19,20] and for the sake of completeness we provide the full assignment, achieved through 2D techniques, of the ¹³C NMR spectrum in the Exp. Sect. Compared with those of **1**, the ¹H and ¹³C NMR spectroscopic signatures of **2**^[24] show changes consistent with the change of an Me to a Br substituent (Scheme 1), that is, the loss of the signals at $\delta = 2.44$ ppm (¹H) and $\delta = 21.4$ ppm (¹³C) arising from the Me group, and shifts of the signals for H^{H3} ($\delta = 7.34$ to 7.65 ppm) and C^{H3} and C^{H4} ($\delta = 129.9$ to 132.4, and 139.4/

139.6 to 123.7 ppm, respectively). The electrospray mass spectrum of **2** exhibits peaks at $m/z = 387.7$, 409.1 and 797.1 assigned to $[\text{M} + \text{H}]^+$, $[\text{M} + \text{Na}]^+$ and $[2\text{M} + \text{Na}]^+$, respectively, with isotope patterns that match those simulated. Ligand **3** was characterized by ¹H and ¹³C NMR spectroscopy (assigned by using COSY, HMQC, HMBC and NOESY techniques); the spectra are consistent with the substitution pattern shown in Scheme 1. Signals arising from the 6-phenyl-2,2'-bipyridine domain are little altered in relation to those observed for **1** and **2**. The base peak in the ESI mass spectrum was observed at $m/z = 467.0$, consistent with $[\text{M} + \text{H}]^+$. Similarly, for **4**, the dominant peak in the ESI mass spectrum ($m/z = 795.7$) arises from the $[\text{M} + \text{H}]^+$ ion. The ¹H and ¹³C NMR spectra for a CDCl₃ solution of **4** were fully assigned by using 2D methods and are consistent with the presence of two diphenylamino substituents (Scheme 1). The electronic absorption spectra of chloroform solutions of **1-4** exhibit intense, high-energy bands arising from $\pi^* \leftarrow \pi$ transitions. The increased values of ϵ_{max} on going from **1-3** to **4** are consistent with the introduction of additional aromatic substituents. All four compounds are emissive ($\lambda_{\text{em}} = 348\text{--}365$ nm for **1-3** and 451 nm for **4**) when irradiated in the UV region corresponding to their most intense absorptions.

Complex Synthesis and Solution Characterization

The complexes $[\text{Ir}(\text{ppy})_2(\text{N}^{\wedge}\text{N})][\text{PF}_6]$ with $\text{N}^{\wedge}\text{N} = \mathbf{1-4}$ were synthesized by the reaction of the dimer $[\text{Ir}(\text{ppy})_2(\mu\text{-Cl})_2]$ ^[25,26] with one of the ligands **1-4** followed by anion exchange by addition of ammonium hexafluoridophosphate (Scheme 2). The electrospray mass spectrum of each isolated complex exhibits a peak envelope corresponding to the $[\text{M} - \text{PF}_6]^+$ ion with an isotope pattern consistent with that simulated.



Scheme 2. Syntheses of $[\text{Ir}(\text{ppy})_2(\text{N}^{\wedge}\text{N})][\text{PF}_6]$ ($\text{L} = \mathbf{1-4}$). Reagents: (i) $\text{N}^{\wedge}\text{N}$, MeOH/CH₂Cl₂ (see Exp. Sect.), (ii) NH₄PF₆. Atom labelling of the [ppy] ligands for NMR spectroscopic assignments.

The complexes were characterized in solution (CD₂Cl₂) by ¹H and ¹³C NMR spectroscopy, the spectra being assigned by using COSY, DEPT, HMQC, HMBC and NOESY techniques. In each $[\text{Ir}(\text{ppy})_2(\text{N}^{\wedge}\text{N})]^+$ cation, the two [ppy]⁻ ligands are non-equivalent because of the lack of a C₂ axis passing through the N[^]N chelate. Well-resolved 500 MHz ¹H NMR spectra were obtained, as exemplified

in Figure 1 for $[\text{Ir}(\text{ppy})_2(\mathbf{3})][\text{PF}_6]$. The proton signals arising from the cyclometallated ring C are distinguished from those of ring A by a NOESY cross-peak between $\text{H}^{\text{G}3}$ and $\text{H}^{\text{C}4}$. As confirmed in the crystallographic study described below, the pendant phenyl ring (ring G, Scheme 1) lies above one of the cyclometallated rings (defined as ring C), leading to close through-space separation of the protons of these rings. In the room-temperature ^1H NMR spectrum it is less easy to unambiguously differentiate between pairs of signals for pyridine rings B and D (Scheme 2). Protons $\text{H}^{\text{F}3}$ and $\text{H}^{\text{F}5}$ are distinguished by the observation of a cross-peak between the signals for $\text{H}^{\text{F}5}$ and $\text{H}^{\text{G}2}$. No $\text{H}^{\text{E}3}$ – $\text{H}^{\text{F}3}$ cross-peak could be observed because of the near overlap of these resonances in the 1D spectrum. The broadening of the signal for $\text{H}^{\text{G}2}$ (Figure 1) is indicative of the slow rotation of the phenyl ring G on the NMR timescale. On cooling a CD_2Cl_2 solution of $[\text{Ir}(\text{ppy})_2(\mathbf{3})][\text{PF}_6]$, the signals arising from $\text{H}^{\text{G}2}$ [$\delta = 6.6$ (br.) ppm at 298 K] and $\text{H}^{\text{G}3}$ ($\delta = 6.78$ ppm at 298 K) collapse, and at 243 K four broad resonances are observed ($\delta = 5.97$ and ca. 7.1 ppm assigned to $\text{H}^{\text{G}2/\text{G}6}$ and $\delta = 6.61$ and 6.89 ppm assigned to $\text{H}^{\text{G}3/\text{G}5}$, Figure 2). The large difference in the chemical shifts of the $\text{H}^{\text{G}2}$ and $\text{H}^{\text{G}6}$ proton signals is consistent with these protons facing into and away from the ring current of arene ring C. Earlier, we noted in the ^1H NMR spectrum recorded at

298 K that it is difficult to differentiate between pairs of proton signals from pyridine rings B and D (Figure 1). However, on cooling from 298 to 243 K one of the pair of signals for $\text{H}^{\text{B}6}$ and $\text{H}^{\text{D}6}$ shifts significantly to lower frequency ($\delta = 6.63$ to 6.47 ppm) and, because of its proximity to the pendant phenyl ring, we assign this signal to $\text{H}^{\text{D}6}$ (Figure 2). All the signals for the protons in the pyridine ring E of coordinated ligand **3** broaden on cooling, but the reason for this is not clear.

The electronic absorption spectra of CD_2Cl_2 solutions of $[\text{Ir}(\text{ppy})_2(\text{N}^{\wedge}\text{N})][\text{PF}_6]$ with $\text{N}^{\wedge}\text{N} = \mathbf{1-4}$ are shown in Figure 3. All the complexes exhibit intense bands in the UV region attributed to ligand-based $\pi^* \leftarrow \pi$ transitions. The similarity of the spectra for $[\text{Ir}(\text{ppy})_2(\mathbf{1})][\text{PF}_6]$, $[\text{Ir}(\text{ppy})_2(\mathbf{2})][\text{PF}_6]$ and $[\text{Ir}(\text{ppy})_2(\mathbf{3})][\text{PF}_6]$ was expected, because the complexes differ only in the peripheral non-aromatic sub-

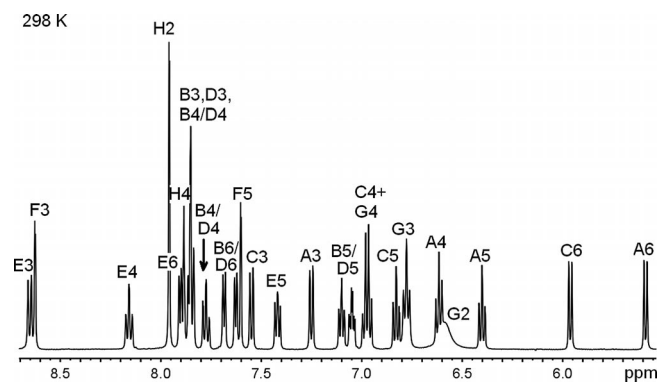


Figure 1. 500 MHz ^1H NMR spectrum of a CD_2Cl_2 solution of $[\text{Ir}(\text{ppy})_2(\mathbf{3})][\text{PF}_6]$ (298 K). Atom labelling as in Schemes 1 and 2.

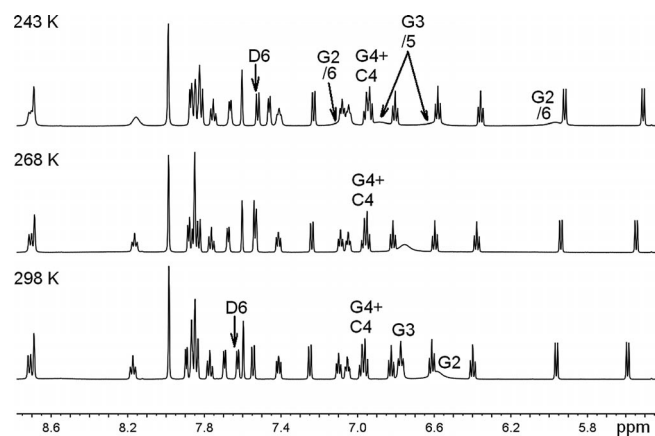


Figure 2. Variable-temperature 500 MHz ^1H NMR spectra of a CD_2Cl_2 solution of $[\text{Ir}(\text{ppy})_2(\mathbf{3})][\text{PF}_6]$.

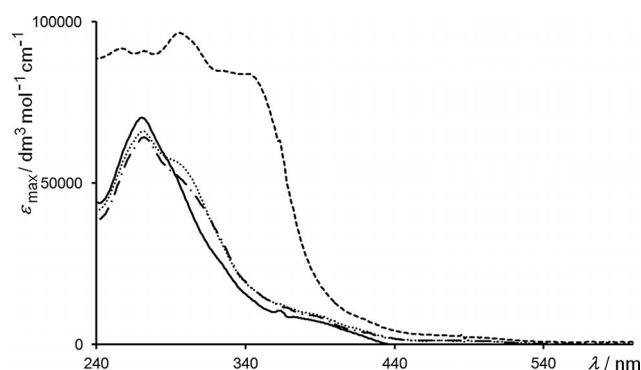


Figure 3. Electronic absorption spectra of CH_2Cl_2 solutions of $[\text{Ir}(\text{ppy})_2(\text{N}^{\wedge}\text{N})][\text{PF}_6]$: $\text{N}^{\wedge}\text{N} = \mathbf{1}$ (---), $\mathbf{2}$ (.....), $\mathbf{3}$ (—) and $\mathbf{4}$ (- - -).

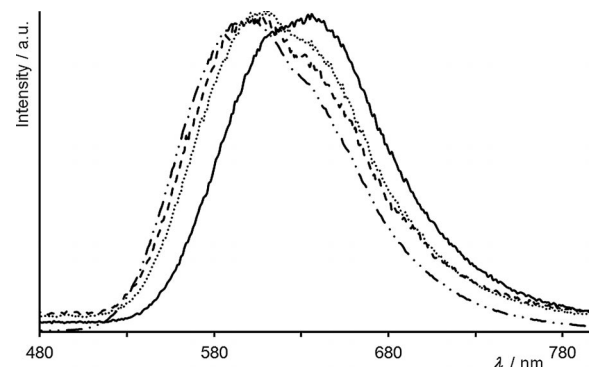


Figure 4. Emission spectra of $[\text{Ir}(\text{ppy})_2(\text{N}^{\wedge}\text{N})][\text{PF}_6]$ (in CH_2Cl_2): $\text{N}^{\wedge}\text{N} = \mathbf{1}$ (---, $\lambda_{\text{ex}} = 279$ nm), $\mathbf{2}$ (....., $\lambda_{\text{ex}} = 229$ nm), $\mathbf{3}$ (—, $\lambda_{\text{ex}} = 232$ nm) and $\mathbf{4}$ (- - -, $\lambda_{\text{ex}} = 229$ nm).

Table 1. Solution photoluminescence spectroscopic data for the hexafluoridophosphate salts of $[\text{Ir}(\text{ppy})_2(\text{N}^{\wedge}\text{N})]^+$ with $\text{N}^{\wedge}\text{N} = \mathbf{1-4}$.^[a]

Complex cation	λ_{ex} [nm]	$\lambda_{\text{em}}^{\text{max}}$ [nm]	$\tau^{\text{[b]}}$ [ns]	ϕ_{PL} [%]
$[\text{Ir}(\text{ppy})_2(\mathbf{1})]^+$	279	600	56.8	19.9
$[\text{Ir}(\text{ppy})_2(\mathbf{2})]^+$	229	608	57.8	14.0
$[\text{Ir}(\text{ppy})_2(\mathbf{3})]^+$	232	635	59.0	11.0
$[\text{Ir}(\text{ppy})_2(\mathbf{4})]^+$	229	604	26.1	5.2

[a] Lifetime and quantum yields were measured in CH_2Cl_2 at room temperature. [b] For lifetime measurements, $\lambda_{\text{ex}} = 300$ nm.

Table 2. Cyclic voltammetric data with respect to Fc/Fc⁺.^[a]

Complex	E_{ox} [V]	E_{red} [V]
[Ir(ppy) ₂ (1)]PF ₆	+0.88 ^{ir} , +1.17/+1.10 ^{qr}	-1.75/-1.68, -2.34 ^{ir} , -2.57 ^{ir}
[Ir(ppy) ₂ (2)]PF ₆	+0.92 ^{ir} , +1.20/+1.14 ^{qr}	-1.67/-1.60, -2.14 ^{ir} , -2.29/-2.23 ^{qr} , -2.57 ^{ir}
[Ir(ppy) ₂ (3)]PF ₆	+0.91 ^{ir} , +1.19/+1.13 ^{qr}	-1.64/-1.57, -2.06 ^{ir} , -2.22 ^{ir} , -2.31/-2.27 ^{qr} , -2.57 ^{ir}
[Ir(ppy) ₂ (4)]PF ₆	+0.92/+0.83, +1.18/+1.12 ^{qr}	-1.46/-1.40, -2.03 ^{ir} , -2.28/-2.20 ^{qr}

[a] Determined in MeCN solutions with [tBu₄N][PF₆] as supporting electrolyte and a scan rate of 0.1 V s⁻¹ (ir = irreversible; qr = quasireversible).

stituents. The enhanced absorption properties of [Ir(ppy)₂(**4**)]PF₆ are consistent with the introduction of six additional arene rings (Scheme 1). The absorption bands tail into the visible region, giving rise to the observed orange colour of the complexes. All four complexes are emissive when excited in the UV region (see caption to Figure 4). The emission maxima for [Ir(ppy)₂(**1**)]PF₆, [Ir(ppy)₂(**2**)]PF₆ and [Ir(ppy)₂(**4**)]PF₆ are similar, whereas the presence of the two bromo substituents in [Ir(ppy)₂(**3**)]PF₆ results in a redshift of ca. 30 nm (Figure 4). Table 1 summarizes the emission data and reveal that the emissions are short-lived with low photoluminescent quantum yields.

All four complexes are electrochemically active, and cyclic voltammetric data are presented in Table 2; unless stated otherwise, processes are reversible. Each of the [Ir(ppy)₂(N^N)]PF₆ complexes with N^N = **1–3** exhibits an irreversible oxidation at ca. +0.9 V, whereas this oxidation is reversible for [Ir(ppy)₂(**4**)]PF₆. A second oxidation process, which is quasi-reversible, is observed for each complex at a more positive potential. A series of ligand-based reductions is exhibited by each complex. The electrochemical behaviour is consistent with that of related complexes.^[27]

Solid-State Structures of the Complexes

The solid-state structures of [Ir(ppy)₂(N^N)]PF₆ for N^N = **1–3** were determined by single-crystal X-ray diffraction, suitable crystals being grown from a CH₂Cl₂ solution of the complex overlaid with Et₂O or by slow evaporation of solvent of a CH₂Cl₂ solution of the complex. The [Ir(ppy)₂(N^N)]⁺ cations are chiral. Although [Ir(ppy)₂(**2**)]PF₆·2CH₂Cl₂ crystallizes in the centrosymmetric space group *P*2₁/*c* with both enantiomers in the unit cell, it is interesting to note that [Ir(ppy)₂(**1**)]PF₆ and [Ir(ppy)₂(**3**)]PF₆ crystallize in the chiral space group *P*2₁2₁2₁. Figures 5–7 present the structures of the [Ir(ppy)₂(**1**)]⁺, [Ir(ppy)₂(**2**)]⁺ and [Ir(ppy)₂(**3**)]⁺ cations, and selected bond lengths and angles are listed in the captions. Each iridium(III) coordination sphere is octahedral with the two cyclometallated [ppy]⁻ ligands bound so that their N donor atoms are in a *trans* arrangement, consistent with related structures (49 entries with {Ir(ppy)₂(N^N)} coordination spheres in the CSD, Conquest version 5.33 with Feb 2012 updates^[28]). The corresponding N–Ir–N bond angle is invariant among the complexes [171.40(18), 171.14(18) and

171.1(3)° for N^N = **1, 2** and **3**, respectively]. As anticipated, the pendant phenyl substituent in each cation is twisted out of the plane of the bpy domain to which it is attached to permit face-to-face π -stacking with the cyclometallated phenyl ring of an adjacent [ppy]⁻ ligand (Figure 8). The angles between the least-squares planes of the bpy unit and the 6-substituted phenyl ring are 69.8(3), 73.4(3) and 63.4(5)° in [Ir(ppy)₂(**1**)]⁺, [Ir(ppy)₂(**2**)]⁺ and [Ir(ppy)₂(**3**)]⁺, respectively. The efficiency of each interaction can be assessed by looking at the angles between the least-squares planes of the two phenyl rings and the separation of their centroids. These parameters are 14.9° and 3.6 Å in [Ir(ppy)₂(**1**)]⁺, 13.9° and 3.5 Å in [Ir(ppy)₂(**2**)]⁺, and 15.3° and 3.6 Å in [Ir(ppy)₂(**3**)]⁺. Although the intercentroid distances are consistent with π -stacking,^[29] the angles between the planes of the rings are not optimal, but are, nonetheless, consistent with those observed in related structures.^[30] The arene ring of each of the tolyl, 4-bromophenyl and 3,5-dibromophenyl substituents is twisted out of the plane of the bpy unit by 36.9° in [Ir(ppy)₂(**1**)]⁺, 26.0° in [Ir(ppy)₂(**2**)]⁺ and 38.0° in [Ir(ppy)₂(**3**)]⁺. This twisting is assumed to be the consequence of packing forces, and it will also minimize repulsive interactions between *ortho*-hydrogen atoms of adjacent rings. Packing interactions in [Ir(ppy)₂(**1**)]PF₆ are dominated by edge-to-face CH \cdots π and CH \cdots F contacts, and there is no intercation face-to-

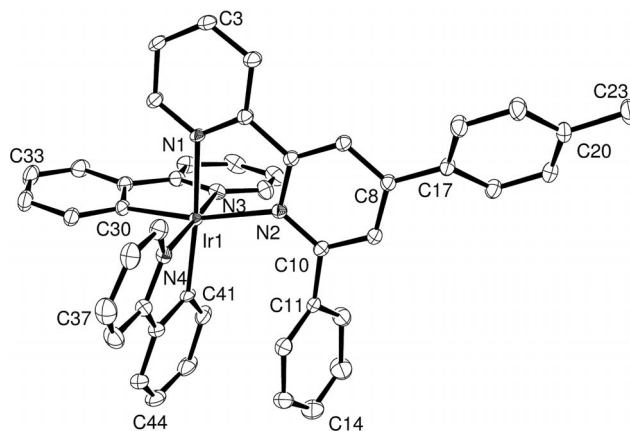


Figure 5. ORTEP representation of the structure of the [Ir(ppy)₂(**1**)]⁺ cation in [Ir(ppy)₂(**1**)]PF₆ (ellipsoids plotted at the 30% probability level and H atoms omitted). Selected bond parameters: Ir1–N1 2.136(4), Ir1–N2 2.213(4), Ir1–C30 2.011(4), Ir1–C41 2.021(4), Ir1–N4 2.043(4), Ir1–N3 2.045(4) Å; N1–Ir1–N2 76.16(15), C41–Ir1–N4 80.1(2), C30–Ir1–N3 80.8(2), C41–Ir1–N1 174.96(19), C30–Ir1–N2 167.51(17), N4–Ir1–N3 171.40(18)°.

face π -stacking. In $[\text{Ir}(\text{ppy})_2(\mathbf{2})][\text{PF}_6]$, pairs of cations associate through short $\text{Br}\cdots\text{Br}$ contacts [$\text{Br}1\cdots\text{Br}1^i$ 3.4617(8) Å; symmetry code: $i = -x, 1 - y, -1 - z$].^[31,32] The $[\text{ppy}]^-$ pyridine ring containing atom N2 engages in a poorly efficient π -stack with the $[\text{ppy}]^-$ phenyl ring containing C22ⁱ (symmetry code: $i = x, 3/2 - y, -1/2 + z$; angle between the least-squares planes of the rings 7.4°, centroid \cdots centroid separation 4.2 Å). Packing forces are dominated by $\text{CH}\cdots\text{F}$ and $\text{CH}\cdots\text{Cl}$ interactions offset by repulsive short $\text{H}\cdots\text{H}$ contacts, particularly those between centrosymmetric pairs of cations ($\text{H}31\cdots\text{H}41^{ii}$ 2.35 Å; symmetry code: $ii = 1 - x, 1 - y, 1 - z$). In $[\text{Ir}(\text{ppy})_2(\mathbf{3})][\text{PF}_6]$, the two bromo substituents are involved in short $\text{Br}\cdots\text{F}$ and $\text{Br}\cdots\pi$ interactions [$\text{Br}2\cdots\text{F}10$ 3.034(9) Å and $\text{Br}1\cdots$ centroid of ring containing

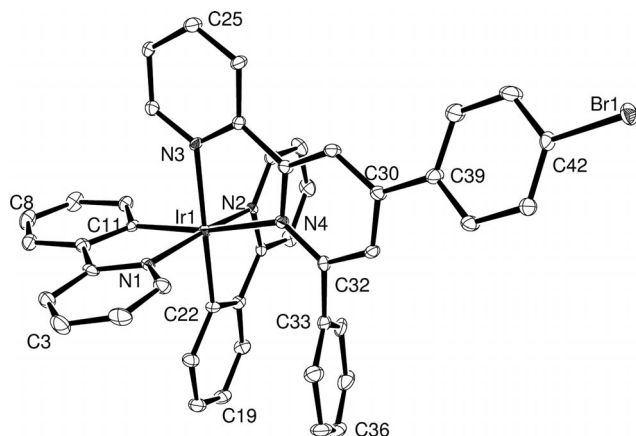


Figure 6. ORTEP representation of the structure of the $[\text{Ir}(\text{ppy})_2(\mathbf{2})]^+$ cation in $[\text{Ir}(\text{ppy})_2(\mathbf{2})][\text{PF}_6]\cdot 2\text{CH}_2\text{Cl}_2$ (ellipsoids plotted at the 30% probability level and H atoms omitted). Selected bond parameters: Ir1–N1 2.039(5), Ir1–N2 2.047(5), Ir1–N3 2.138(5), Ir1–N4 2.223(5), Ir1–C11 1.996(5), Ir1–C22 2.035(6), C42–Br1 1.894(6) Å; N3–Ir1–N4 75.99(18), N1–Ir1–C11 80.7(2), N2–Ir1–C22 79.9(2), N1–Ir1–N2 171.14(18), N4–Ir1–C11 168.27(19), N3–Ir1–C22 174.8(2)°.

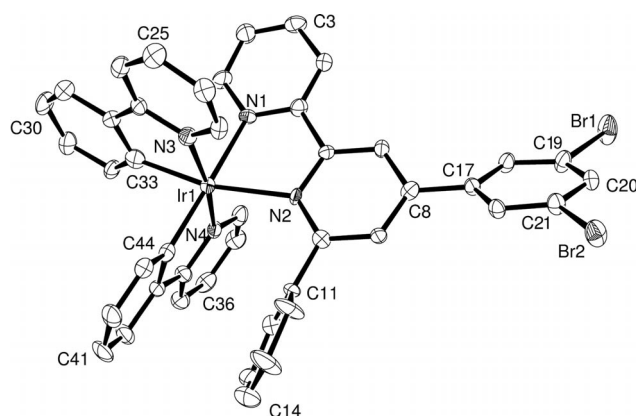


Figure 7. ORTEP representation of the structure of the $[\text{Ir}(\text{ppy})_2(\mathbf{3})]^+$ cation in $[\text{Ir}(\text{ppy})_2(\mathbf{3})][\text{PF}_6]$ (ellipsoids plotted at the 30% probability level and H atoms omitted). Selected bond parameters: Ir1–C44 2.014(10), Ir1–C33 2.029(10), Ir1–N4 2.032(8), Ir1–N3 2.045(8), Ir1–N1 2.146(7), Ir1–N 2.253(6), C19–Br1 1.908(9), C21–Br2 1.891(9) Å; N1–Ir1–N2 75.3(3), C33–Ir1–N3 80.5(5), C44–Ir1–N4 81.1(4), N4–Ir1–N3 171.1(3), C33–Ir1–N2 167.2(4), C44–Ir1–N1 177.2(4)°.

N3ⁱ 3.54 Å with closest contacts of $\text{Br}1\cdots\text{C}25^i$ 3.40(1) and $\text{Br}1\cdots\text{C}26^i$ 3.54(1) Å; symmetry code: $i = x, 1 + y, z$). Intercation face-to-face π -stacking does not play an important role in crystal packing, except for a poorly efficient interaction between pairs of $[\text{ppy}]^-$ ligands containing atoms C33 and N4ⁱⁱ (symmetry code: $ii = 2 - x, -1/2 + y, 3/2 - z$; angle between least-squares planes of rings 17.6°, centroid \cdots centroid separation 3.9 Å). Edge-to-face $\text{CH}\cdots\pi$ and $\text{CH}\cdots\text{F}$ contacts are the dominant packing interactions.

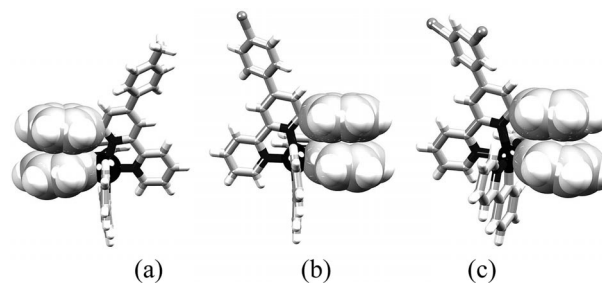


Figure 8. Intracation face-to-face π -stacking in (a) $[\text{Ir}(\text{ppy})_2(\mathbf{1})]^+$, (b) $[\text{Ir}(\text{ppy})_2(\mathbf{2})]^+$ and (c) $[\text{Ir}(\text{ppy})_2(\mathbf{3})]^+$.

Solid-State Photophysical Properties and Electroluminescent Devices

The solid-state photoluminescence emission spectra of thin films containing $[\text{Ir}(\text{ppy})_2(\text{N}^{\wedge}\text{N})][\text{PF}_6]$ ($\text{N}^{\wedge}\text{N} = \mathbf{1-4}$) and the ionic liquid 1-butyl-3-methylimidazolium hexafluoridophosphate (IL) in an $[\text{Ir}(\text{ppy})_2(\text{N}^{\wedge}\text{N})]^+/\text{IL}$ molar ratio of 4:1 are displayed in Figure 9a. The photoluminescence spectra are similar to those obtained for the complexes in CD_2Cl_2 solution (Figure 4). The emission peak from $[\text{Ir}(\text{ppy})_2(\mathbf{3})][\text{PF}_6]$ at 629 nm is the most redshifted; emission maxima were observed for $[\text{Ir}(\text{ppy})_2(\mathbf{2})][\text{PF}_6]$, $[\text{Ir}(\text{ppy})_2(\mathbf{4})][\text{PF}_6]$ and $[\text{Ir}(\text{ppy})_2(\mathbf{1})][\text{PF}_6]$ at 608, 604 and 601 nm, respectively. The similarity of the solid- and solution-based data demonstrates that the excited state is not severely affected by the environment as has been observed in other systems.^[33] The photoluminescent quantum yields (PLQY) of the complexes in the configuration described above are 0.15, 0.11, 0.13 and 0.08 for $[\text{Ir}(\text{ppy})_2(\mathbf{1})][\text{PF}_6]$, $[\text{Ir}(\text{ppy})_2(\mathbf{2})][\text{PF}_6]$, $[\text{Ir}(\text{ppy})_2(\mathbf{3})][\text{PF}_6]$ and $[\text{Ir}(\text{ppy})_2(\mathbf{4})][\text{PF}_6]$, respectively.

The electroluminescence of LECs prepared from the four complexes in the layer composition as described above is shown in Figure 9b. The emission band maxima are found at 588, 597 and 595 nm for the complexes $[\text{Ir}(\text{ppy})_2(\mathbf{1})][\text{PF}_6]$, $[\text{Ir}(\text{ppy})_2(\mathbf{2})][\text{PF}_6]$ and $[\text{Ir}(\text{ppy})_2(\mathbf{4})][\text{PF}_6]$, respectively, whereas for $[\text{Ir}(\text{ppy})_2(\mathbf{3})][\text{PF}_6]$, the emission is at 620 nm. The slightly blueshifted emissions with respect to the photoluminescence spectra may be due to optical effects caused by the presence of the metal top electrode and specific regions in the film where the electrons and holes recombine and the light originates. This leads to a different optical path for the generated photons, which may explain the slight difference between PL and EL emission. The LECs were driven by using a recently reported method of a pulsed

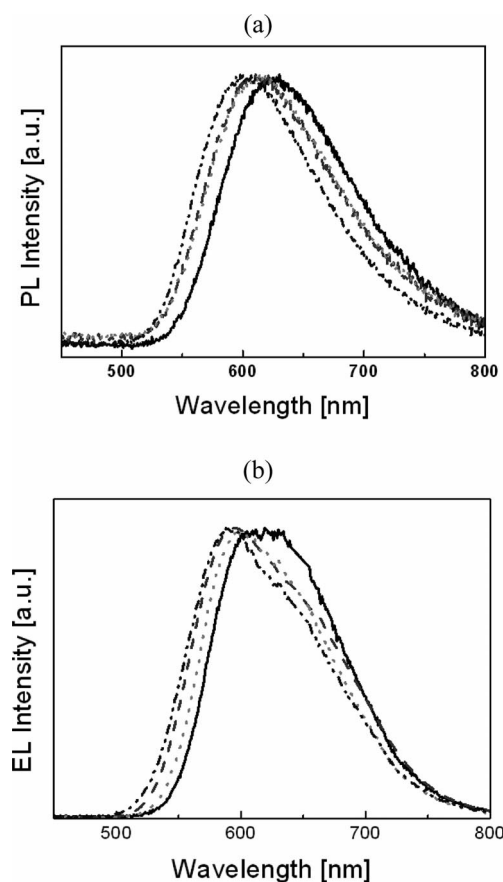


Figure 9. (a) Photoluminescence spectra for $[\text{Ir}(\text{ppy})_2(\text{N}^{\wedge}\text{N})][\text{PF}_6]/\text{IL}$ (4:1) in the solid state and (b) electroluminescence spectra for ITO/PEDOT:PSS/ $[\text{Ir}(\text{ppy})_2(\text{N}^{\wedge}\text{N})][\text{PF}_6]/\text{IL}$ (4:1)/Al LECs under a bias of 4 V [$\text{N}^{\wedge}\text{N} = 1$ (\cdots), 2 ($\cdots\cdots$), 3 (---) and 4 (- - -)].

current with an average current density of 100 A m^{-2} using a block wave at a frequency of 1000 Hz and a duty cycle of 50%.^[34] These driving conditions were selected, because current driving leads to fast turn-on times, and pulsed driving stabilizes the doped regions leading to increased lifetimes. More importantly, the lifetimes observed with this driving method are linked to the intrinsic stability of the device and complex used.

Typical performances obtained with the LECs prepared from $[\text{Ir}(\text{ppy})_2(\mathbf{1})][\text{PF}_6]$, $[\text{Ir}(\text{ppy})_2(\mathbf{2})][\text{PF}_6]$, $[\text{Ir}(\text{ppy})_2(\mathbf{3})][\text{PF}_6]$ or $[\text{Ir}(\text{ppy})_2(\mathbf{4})][\text{PF}_6]$ are presented in Figure 10 and are summarized in Table 3. As LECs are dynamic systems, the field-induced ionic movement reduces the injection barrier for holes and electrons and, as a consequence, luminance increases as the voltage decreases. The decrease in voltage

implies it is easier to maintain the pre-set average current density due to the reduced injection barrier. An important parameter of LECs is the turn-on time (t_{on}), in this work defined as the time to reach 75 cd m^{-2} . All devices turn on within 2 h of operation, which is primarily due to the selected mode of operation for the LECs. Interestingly, the lowest t_{on} is reached for the LEC using $[\text{Ir}(\text{ppy})_2(\mathbf{2})][\text{PF}_6]$, which shows 85 cd m^{-2} instantly upon operation. The LECs using $[\text{Ir}(\text{ppy})_2(\mathbf{3})][\text{PF}_6]$ and $[\text{Ir}(\text{ppy})_2(\mathbf{4})][\text{PF}_6]$ have t_{on} values of 0.9 and 0.4 h, respectively, whereas the LEC using $[\text{Ir}(\text{ppy})_2(\mathbf{1})][\text{PF}_6]$ needs 2 h to reach 75 cd m^{-2} . The luminance continues to increase for the LECs, and – as the current density is constant – the device efficacy is easily deduced by dividing the luminance by the constant current density (100 A m^{-2}).

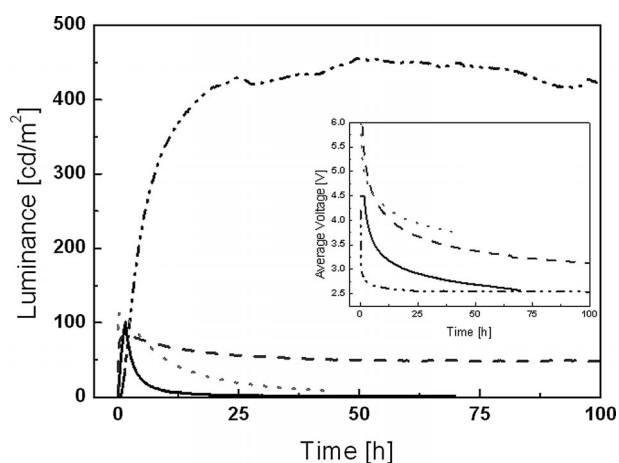


Figure 10. Luminance and average voltage (inset) versus time for ITO/PEDOT:PSS/ $[\text{Ir}(\text{ppy})_2(\text{N}^{\wedge}\text{N})][\text{PF}_6]/\text{IL}$ (4:1)/Al LEC devices under an average pulsed current of 100 A m^{-2} (1000 Hz and 50% duty cycle). $\text{N}^{\wedge}\text{N} = 1$ (\cdots), 2 ($\cdots\cdots$), 3 (---) and 4 (- - -).

The initial driving voltages applied are an indication of the ionic conductivity of the film as the displacement of ions is required to reduce the injection barrier for electrons and holes. The voltage applied increases going from the LEC using $[\text{Ir}(\text{ppy})_2(\mathbf{1})][\text{PF}_6]$, $[\text{Ir}(\text{ppy})_2(\mathbf{3})][\text{PF}_6]$, $[\text{Ir}(\text{ppy})_2(\mathbf{4})][\text{PF}_6]$ and finally $[\text{Ir}(\text{ppy})_2(\mathbf{2})][\text{PF}_6]$. In particular, the large difference in driving voltage for LECs using $[\text{Ir}(\text{ppy})_2(\mathbf{1})][\text{PF}_6]$ and $[\text{Ir}(\text{ppy})_2(\mathbf{2})][\text{PF}_6]$ is peculiar as there is only a small difference in the chemical structure of the bpy-based ligand (Scheme 1).

The stabilities of the different devices cannot easily be compared as the luminance levels are quite different. However, one observes that the devices using the complexes with

Table 3. Performance for ITO/PEDOT:PSS/ $[\text{Ir}(\text{ppy})_2(\text{bpy})][\text{PF}_6]/\text{IL}$ (4:1)/Al LEC devices [$\text{N}^{\wedge}\text{N} = 1$ (\cdots), 2 ($\cdots\cdots$), 3 (---) and 4 (- - -)] driven at a pulsed current with an average current density of 100 A m^{-2} by using a block wave at a frequency of 1000 Hz and a duty cycle of 50%.

Complex cation	t_{on} [h]	L_{max} [cd m^{-2}]	$t_{1/2}$ [h]	Efficacy [cd A^{-1}]	PLQY [%]	Power efficiency [lm W^{-1}]	EQE [%]
$[\text{Ir}(\text{ppy})_2(\mathbf{1})]^+$	2.0	455	530	4.4	14.7	2.72	2.12
$[\text{Ir}(\text{ppy})_2(\mathbf{2})]^+$	instant	115	8.3	1.1	11.4	0.33	0.60
$[\text{Ir}(\text{ppy})_2(\mathbf{3})]^+$	0.9	101	2.9	1.4	12.9	0.25	0.95
$[\text{Ir}(\text{ppy})_2(\mathbf{4})]^+$	0.4	83	250	0.8	7.76	0.25	0.43

the bromine substituents have a significantly lower stability than the LECs using complexes containing ligand $N^{\wedge}N = \mathbf{1}$ and $\mathbf{4}$. This would suggest that the presence of Br substituents is not beneficial for the operation of LECs.

Conclusions

As a part of our systematic investigation of iridium complexes for incorporation into LECs, we have prepared and characterized four iridium(III) complexes $[\text{Ir}(\text{ppy})_2(\text{N}^{\wedge}\text{N})][\text{PF}_6]$ in which $\text{N}^{\wedge}\text{N}$ is a 4,6-diphenyl-2,2'-bipyridine and the 4-phenyl ring is substituted at either the *para* or *meta* positions with electron-releasing or -withdrawing substituents (Scheme 1). The $\text{N}^{\wedge}\text{N}$ ligands were designed to permit intracation face-to-face π -stacking between the cyclometallated phenyl ring of one $[\text{ppy}]^-$ ligand and the pendant 6-phenyl substituent of the co-ligand. X-ray diffraction data for three of the complexes confirmed this solid-state feature. In solution, the complexes are short-lived emitters ($\lambda_{\text{em}} = 600\text{--}608\text{ nm}$ for $\text{N}^{\wedge}\text{N} = \mathbf{1}$, $\mathbf{2}$ and $\mathbf{4}$, and 635 nm for $\text{N}^{\wedge}\text{N} = \mathbf{3}$), and the solid-state photoluminescence emission spectra of thin films of the complexes are little different from those in CH_2Cl_2 solution. Evaluation of the performances of the iridium(III) complexes in LECs revealed that the electroluminescence spectra are slightly blueshifted with respect to the photoluminescence spectra, and the LEC turn-on times range from instantaneous for $\text{N}^{\wedge}\text{N} = \mathbf{2}$ to 2 h for $\text{N}^{\wedge}\text{N} = \mathbf{1}$. The device data suggest that the incorporation of Br substituents into the $\text{N}^{\wedge}\text{N}$ co-ligand are not beneficial and confirm our general belief that halogens should be avoided as substituents in ligands designed for use in LECs.

Experimental Section

General: See the Supporting Information.

Compound 1: The ligand was prepared in a manner similar to a literature method^[20] but by adapting it to employ the solventless protocol of Cave and Raston^[23] (see the Supporting Information). The CDCl_3 solution ^1H NMR spectroscopic data are in agreement with those reported in the literature.^[19,20] The following characterization data have not previously been reported for $\mathbf{1}$. M.p. $125\text{ }^\circ\text{C}$. ^{13}C NMR (126 MHz, CDCl_3): $\delta = 157.4$ ($\text{C}^{\text{F}6}$), 156.0 ($\text{C}^{\text{E}2/\text{F}2}$), 150.4 ($\text{C}^{\text{F}4}$), 148.4 ($\text{C}^{\text{E}6}$), 139.6 ($\text{C}^{\text{G}1/\text{H}4}$), 139.4 ($\text{C}^{\text{G}1/\text{H}4}$), 138.0 ($\text{C}^{\text{E}4}$), 135.7 ($\text{C}^{\text{H}1}$), 129.9 ($\text{C}^{\text{H}3}$), 129.3 ($\text{C}^{\text{G}4}$), 128.9 ($\text{C}^{\text{G}3}$), 127.3 ($\text{C}^{\text{G}2/\text{H}2}$), 127.2 ($\text{C}^{\text{G}2/\text{H}2}$), 124.1 ($\text{C}^{\text{E}5}$), 122.1 ($\text{C}^{\text{E}3}$), 118.7 ($\text{C}^{\text{F}5}$), 117.7 ($\text{C}^{\text{F}3}$), 21.4 (CH_3) ppm. UV/Vis (CHCl_3 , $6.82 \times 10^{-6}\text{ mol dm}^{-3}$): $\lambda_{\text{max}}(\epsilon) = 264$ (46000), 315 nm ($10000\text{ dm}^3\text{ mol}^{-1}\text{ cm}^{-1}$); emission (CHCl_3 , $6.82 \times 10^{-6}\text{ mol dm}^{-3}$, $\lambda_{\text{ex}} = 264\text{ nm}$): $\lambda_{\text{em}} = 348, 359\text{ nm}$. MS (ESI): $m/z = 323.2$ [$\text{M} + \text{H}$] $^+$ (calcd. 323.2), 345.1 [$\text{M} + \text{Na}$] $^+$ (calcd. 345.1), 667.2 [$2\text{M} + \text{Na}$] $^+$ (calcd. 667.3).

Compound 2: KOH (1.09 g, 19.5 mmol) was dissolved in MeOH (50 mL) and H_2O (10 mL) whilst stirring in an ice bath, and acetophenone (1.948 g, 16.2 mmol) and 4-bromobenzaldehyde (3.00 g, 16.2 mmol) were added slowly. After stirring for 1 h, a white precipitate formed. The crude product was transferred to a mortar and combined with solid NaOH (650 mg, 16.2 mmol), and 2-acet-

ylpyridine (1.964 g, 16.2 mmol) was then added. The mixture was ground to a paste and then a solid. After drying in a desiccator, the solid was milled to give a beige powder. This was dissolved in a solution of NH_4OAc (12.5 g, 162 mmol) in PEG-300 (200 mL) and the mixture heated at reflux for 18 h. Water (100 mL) was added to the cooled mixture and the sticky product was separated, washed with water ($50 \times 2\text{ mL}$) and dissolved in Et_2O . Removal of the solvent gave a brown solid, which was dissolved in CH_2Cl_2 and washed with aqueous NaHCO_3 and water. The organic layer was dried with MgSO_4 , filtered, and the solvents were evaporated to dryness to give a brown solid, which was purified by column chromatography (silica, CH_2Cl_2 changing to $\text{CH}_2\text{Cl}_2/\text{MeOH}$, 100:1; then alumina, changing to $\text{CH}_2\text{Cl}_2/\text{MeOH}$, 100:1). Compound $\mathbf{2}$ was isolated as a pale-yellow solid (1.24 g, 3.20 mmol, 19.7%). M.p. $147\text{ }^\circ\text{C}$. ^1H NMR (500 MHz, CDCl_3): $\delta = 8.76$ (d, $J = 4.5\text{ Hz}$, 1 H, $\text{H}^{\text{E}6}$), 8.73 (d, $J = 8.0\text{ Hz}$, 1 H, $\text{H}^{\text{E}3}$), 8.70 (s, 1 H, $\text{H}^{\text{F}3}$), 8.19 (d, $J = 7.2\text{ Hz}$, 2 H, $\text{H}^{\text{G}2}$), 7.95 (m, 2 H, $\text{H}^{\text{F}5+\text{E}4}$), 7.73 (d, $J = 8.5\text{ Hz}$, 2 H, $\text{H}^{\text{H}2}$), 7.65 (d, $J = 8.5\text{ Hz}$, 2 H, $\text{H}^{\text{H}3}$), 7.54 (t, $J = 7.4\text{ Hz}$, 2 H, $\text{H}^{\text{G}3}$), 7.47 (t, $J = 7.3\text{ Hz}$, 1 H, $\text{H}^{\text{G}4}$), 7.42 (m, 1 H, $\text{H}^{\text{E}5}$) ppm. ^{13}C NMR (126 MHz, CDCl_3): $\delta = 157.7$ ($\text{C}^{\text{F}6}$), 155.5 ($\text{C}^{\text{E}2/\text{F}2}$), 155.2 ($\text{C}^{\text{E}2/\text{F}2}$), 149.3 ($\text{C}^{\text{F}4}$), 148.2 ($\text{C}^{\text{E}6}$), 139.2 ($\text{C}^{\text{G}1}$), 138.3 ($\text{C}^{\text{E}4}$), 137.5 ($\text{C}^{\text{H}1}$), 132.4 ($\text{C}^{\text{H}3}$), 129.5 ($\text{C}^{\text{G}4}$), 129.0 ($\text{C}^{\text{H}2/\text{G}3}$), 128.9 ($\text{C}^{\text{H}2/\text{G}3}$), 127.2 ($\text{C}^{\text{G}2}$), 124.4 ($\text{C}^{\text{E}5}$), 123.7 ($\text{C}^{\text{H}4}$), 122.3 ($\text{C}^{\text{E}3}$), 118.6 ($\text{C}^{\text{F}5}$), 117.7 ($\text{C}^{\text{F}3}$) ppm. UV/Vis (CHCl_3 , $5.68 \times 10^{-6}\text{ mol dm}^{-3}$): $\lambda_{\text{max}}(\epsilon) = 265$ (43000), 312 nm ($8000\text{ dm}^3\text{ mol}^{-1}\text{ cm}^{-1}$); emission (CHCl_3 , $4.75 \times 10^{-5}\text{ mol dm}^{-3}$, $\lambda_{\text{ex}} = 312\text{ nm}$): $\lambda_{\text{em}} = 354, 363\text{ nm}$. MS (ESI): $m/z = 387.7$ [$\text{M} + \text{H}$] $^+$ (calcd. 387.1), 409.1 [$\text{M} + \text{Na}$] $^+$ (calcd. 409.0), 797.1 [$2\text{M} + \text{Na}$] $^+$ (calcd. 797.1). $\text{C}_{22}\text{H}_{15}\text{BrN}_2$ (387.28): calcd. C 68.23, H 3.90, N 7.23; found C 68.08, H 4.18, N 6.90.

Compound 3: Ligand $\mathbf{3}$ was prepared in a manner similar to that for $\mathbf{2}$ (see the Supporting Information) and was isolated as a white solid (26%). M.p. $187\text{ }^\circ\text{C}$. ^1H NMR (500 MHz, CDCl_3): $\delta = 8.74$ (d, $J = 4.8\text{ Hz}$, 1 H, $\text{H}^{\text{E}6}$), 8.69 (d, $J = 8.0\text{ Hz}$, 1 H, $\text{H}^{\text{E}3}$), 8.58 (s, 1 H, $\text{H}^{\text{F}3}$), 8.19 (d, $J = 7.1\text{ Hz}$, 2 H, $\text{H}^{\text{G}2}$), 7.89 (m, 4 H, $\text{H}^{\text{H}2+\text{E}4+\text{F}5}$), 7.75 (t, $J = 1.6\text{ Hz}$, 1 H, $\text{H}^{\text{H}4}$), 7.54 (t, $J = 7.4\text{ Hz}$, 2 H, $\text{H}^{\text{G}3}$), 7.48 (t, $J = 7.3\text{ Hz}$, 1 H, $\text{H}^{\text{G}4}$), 7.39 (m, 1 H, $\text{H}^{\text{E}5}$) ppm. ^{13}C NMR (126 MHz, CDCl_3): $\delta = 157.7$ ($\text{C}^{\text{F}6}$), 156.3 ($\text{C}^{\text{F}2}$), 155.7 ($\text{C}^{\text{E}2}$), 148.9 ($\text{C}^{\text{E}6}$), 147.6 ($\text{C}^{\text{F}4}$), 142.4 ($\text{C}^{\text{H}1}$), 139.0 ($\text{C}^{\text{G}1}$), 137.5 ($\text{C}^{\text{E}4}$), 134.5 ($\text{C}^{\text{H}4}$), 129.6 ($\text{C}^{\text{G}4}$), 129.2 ($\text{C}^{\text{H}2}$), 129.0 ($\text{C}^{\text{G}3}$), 127.2 ($\text{C}^{\text{G}2}$), 124.3 ($\text{C}^{\text{E}5}$), 123.8 ($\text{C}^{\text{H}3}$), 121.9 ($\text{C}^{\text{E}3}$), 118.4 ($\text{C}^{\text{F}5}$), 117.5 ($\text{C}^{\text{F}3}$) ppm. UV/Vis (CHCl_3 , $5.15 \times 10^{-6}\text{ mol dm}^{-3}$): $\lambda_{\text{max}}(\epsilon) = 240$ (47000), 254 (45000), 316 nm ($9000\text{ dm}^3\text{ mol}^{-1}\text{ cm}^{-1}$); emission (CHCl_3 , $5.15 \times 10^{-5}\text{ mol dm}^{-3}$, $\lambda_{\text{ex}} = 255\text{ nm}$): $\lambda_{\text{em}} = 365\text{ nm}$. MS (ESI): $m/z = 467.0$ [$\text{M} + \text{H}$] $^+$ (calcd. 467.0), 466.17 : calcd. C 56.68, H 3.03, N 6.01; found C 56.59, H 3.04, N 6.02.

Compound 4: Compound $\mathbf{3}$ (795 mg, 1.71 mmol), 4-(diphenylamino)phenylboronic acid (1.06 g, 3.67 mmol) and Na_2CO_3 (730 mg, 6.9 mmol) were dissolved in toluene (200 mL) and water (50 mL). The reaction mixture was degassed with N_2 for 30 min, and then $[\text{Pd}(\text{PPh}_3)_4]$ (197 mg, 0.17 mmol) was added. The mixture was heated at reflux in the dark for 5 d. After cooling, the two phases were separated, and the organic layer was washed with H_2O ($2 \times 50\text{ mL}$), dried with MgSO_4 and filtered. Removal of the solvent gave a yellow oil, which was purified by column chromatography (silica, toluene/ethyl acetate, 20:1; then alumina, toluene/cyclohexane, 1:1). Ligand $\mathbf{4}$ was isolated as a white powder (1.09 g, 1.40 mmol, 81.9%). M.p. $255\text{ }^\circ\text{C}$. ^1H NMR (500 MHz, CDCl_3): $\delta = 8.80$ (s, 1 H, $\text{H}^{\text{F}3}$), 8.74 (overlapping d, 2 H, $\text{H}^{\text{E}3+\text{E}6}$), 8.25 (d, $J = 7.2\text{ Hz}$, 2 H, $\text{H}^{\text{G}2}$), 8.10 (s, 1 H, $\text{H}^{\text{F}5}$), 7.95 (s, 2 H, $\text{H}^{\text{H}2}$), 7.91 (t, $J = 7.9\text{ Hz}$, 1 H, $\text{H}^{\text{E}4}$), 7.86 (s, 1 H, $\text{H}^{\text{H}4}$), 7.63 (d, $J = 8.6\text{ Hz}$, 4 H, $\text{H}^{\text{H}2}$), 7.56 (t, $J = 7.5\text{ Hz}$, 2 H, $\text{H}^{\text{G}3}$), 7.48 (t, $J = 7.3\text{ Hz}$, 1 H, $\text{H}^{\text{G}4}$), 7.39 (m, 1 H, $\text{H}^{\text{E}5}$), 7.30 (t, $J = 7.9\text{ Hz}$, 8 H, $\text{H}^{\text{J}3}$), 7.20

FULL PAPER

(overlapping d, 12 H, H^{13+J2}), 7.07 (t, $J = 7.3$ Hz, 4 H, H^{J4}) ppm. ^{13}C NMR (126 MHz, CDCl_3): $\delta = 157.4$ ($\text{C}^{\text{F}6}$), 156.2 ($\text{C}^{\text{E}2+\text{F}2}$), 150.6 ($\text{C}^{\text{F}4}$), 148.8 ($\text{C}^{\text{E}6}$), 147.7 ($\text{C}^{14+\text{J}1}$), 142.3 ($\text{C}^{\text{H}3}$), 139.9 ($\text{C}^{\text{H}1}$), 139.5 ($\text{C}^{\text{G}1}$), 137.5 ($\text{C}^{\text{E}4}$), 134.8 ($\text{C}^{\text{I}1}$), 129.5 ($\text{C}^{\text{J}3}$), 129.3 ($\text{C}^{\text{G}4}$), 128.9 ($\text{C}^{\text{G}3}$), 128.2 ($\text{C}^{\text{I}2}$), 127.3 ($\text{C}^{\text{G}2}$), 126.0 ($\text{C}^{\text{H}4}$), 124.6 ($\text{C}^{\text{J}2}$), 124.4 ($\text{C}^{\text{H}2}$), 124.1 ($\text{C}^{\text{E}5}$), 124.0 ($\text{C}^{\text{I}3}$), 123.2 ($\text{C}^{\text{J}4}$), 121.9 ($\text{C}^{\text{E}3}$), 118.9 ($\text{C}^{\text{F}5}$), 118.0 ($\text{C}^{\text{F}3}$) ppm. UV/Vis (CHCl_3 , 4.91×10^{-5} mol dm $^{-3}$): λ_{max} (ϵ) = 247 (76000), 312 nm (60000 dm 3 mol $^{-1}$ cm $^{-1}$); emission (CHCl_3 , 4.91×10^{-5} mol dm $^{-3}$, $\lambda_{\text{ex}} = 320$ nm): $\lambda_{\text{em}} = 451$ nm. MS (ESI): $m/z = 795.7$ [$\text{M} + \text{H}$] $^+$ (calcd. 795.3). $\text{C}_{58}\text{H}_{42}\text{N}_4$ (795.00): calcd. C 87.63, H 5.32, N 7.05; found C 87.35, H 5.58, N 7.01.

[Ir(ppy) $_2$ (1)]PF $_6$]: A yellow suspension of $[\text{Ir}_2(\text{ppy})_4(\mu\text{-Cl})_2]$ (55.4 mg, 0.052 mmol) and **1** (33.2 mg, 0.103 mmol) in MeOH was placed in a vial in a microwave reactor at 120 °C for 2 h. The orange solution was cooled to room temperature, and an excess of NH_4PF_6 was added. The mixture was stirred for 30 min and was then concentrated to dryness. Purification by column chromatography (alumina, CH_2Cl_2 changing to $\text{CH}_2\text{Cl}_2/\text{MeOH}$, 100:1; then silica, CH_2Cl_2 changing to $\text{CH}_2\text{Cl}_2/\text{MeOH}$, 100:1) yielded $[\text{Ir}(\text{ppy})_2\text{-}(\mathbf{1})]\text{PF}_6$ as an orange solid (75 mg, 0.077 mmol, 75%). ^1H NMR (500 MHz, CD_2Cl_2): $\delta = 8.70$ (d, $J = 1.5$ Hz, 1 H, $\text{H}^{\text{F}3}$), 8.65 (d, $J = 8.2$ Hz, 1 H, $\text{H}^{\text{E}3}$), 8.14 (td, $J = 8.1$, 1.0 Hz, 1 H, $\text{H}^{\text{E}4}$), 7.90 (d, $J = 4.9$ Hz, 1 H, $\text{H}^{\text{E}6}$), 7.85 (overlapping m, 3 H, $\text{H}^{\text{B}3+\text{B}4+\text{D}3}$), 7.81 (d, $J = 8.3$ Hz, 2 H, $\text{H}^{\text{H}2}$), 7.76 (t, $J = 8.2$ Hz, 1 H, $\text{H}^{\text{D}4}$), 7.71 (d, $J = 5.7$ Hz, 1 H, $\text{H}^{\text{B}6}$), 7.68 (d, $J = 1.6$ Hz, 1 H, $\text{H}^{\text{F}5}$), 7.61 (d, $J = 5.4$ Hz, 1 H, $\text{H}^{\text{D}6}$), 7.54 (d, $J = 7.6$ Hz, 1 H, $\text{H}^{\text{C}3}$), 7.42 (d, $J = 8.4$ Hz, 2 H, $\text{H}^{\text{H}3}$), 7.39 (d, $J = 6.4$ Hz, 1 H, $\text{H}^{\text{E}5}$), 7.25 (d, $J = 7.6$ Hz, 1 H, $\text{H}^{\text{A}3}$), 7.08 (m, 1 H, $\text{H}^{\text{D}5}$), 7.04 (m, 1 H, $\text{H}^{\text{B}5}$), 6.96 (overlapping m, 2 H, $\text{H}^{\text{C}4+\text{G}4}$), 6.83 (t, $J = 7.4$ Hz, 1 H, $\text{H}^{\text{C}5}$), 6.76 (t, $J = 7.5$ Hz, 2 H, $\text{H}^{\text{G}3}$), 6.61 (t, $J = 7.5$ Hz, 1 H, $\text{H}^{\text{A}4}$), 6.6 (br., $\text{H}^{\text{G}2}$), 6.40 (t, $J = 7.4$ Hz, 1 H, $\text{H}^{\text{A}5}$), 5.98 (d, $J = 7.7$ Hz, 1 H, $\text{H}^{\text{C}6}$), 5.60 (d, $J = 7.6$ Hz, 1 H, $\text{H}^{\text{A}6}$), 2.45 (s, 3 H, Me) ppm. ^{13}C NMR (126 MHz, CD_2Cl_2): $\delta = 169.4$ ($\text{C}^{\text{B}2}$), 167.8 ($\text{C}^{\text{D}2}$), 166.4 ($\text{C}^{\text{F}6}$), 157.7 ($\text{C}^{\text{E}2/\text{F}2}$), 157.5 ($\text{C}^{\text{E}2/\text{F}2}$), 151.6 ($\text{C}^{\text{A}1}$), 150.9 ($\text{C}^{\text{E}6}$), 149.5 ($\text{C}^{\text{B}6/\text{D}6}$), 149.3 ($\text{C}^{\text{B}6/\text{D}6}$), 147.5 ($\text{C}^{\text{C}1}$), 143.5 ($\text{C}^{\text{C}2}$), 143.3 ($\text{C}^{\text{A}2}$), 142.5 ($\text{C}^{\text{H}4}$), 139.8 ($\text{C}^{\text{E}4}$), 138.7 ($\text{C}^{\text{B}4/\text{D}4}$), 138.5 ($\text{C}^{\text{B}4/\text{D}4}$), 138.4 ($\text{C}^{\text{G}1}$), 132.6 ($\text{C}^{\text{H}1}$), 131.9 ($\text{C}^{\text{A}6}$), 131.3 ($\text{C}^{\text{C}5}$), 130.9 ($\text{C}^{\text{H}3}$), 130.8 ($\text{C}^{\text{C}6}$), 130.1 ($\text{C}^{\text{A}5}$), 129.5 ($\text{C}^{\text{G}4}$), 128.4 ($\text{C}^{\text{G}3}$), 128.3 ($\text{C}^{\text{E}5}$), 127.9 ($\text{C}^{\text{G}2}$), 127.8 ($\text{C}^{\text{H}2}$), 127.3 ($\text{C}^{\text{F}5}$), 125.6 ($\text{C}^{\text{E}3}$), 125.1 ($\text{C}^{\text{A}3/\text{C}3}$), 125.0 ($\text{C}^{\text{A}3/\text{C}3}$), 123.9 ($\text{C}^{\text{D}5}$), 123.3 ($\text{C}^{\text{C}4}$), 122.9 ($\text{C}^{\text{B}5}$), 121.3 ($\text{C}^{\text{A}4}$), 120.9 ($\text{C}^{\text{F}3}$), 120.4 ($\text{C}^{\text{B}3/\text{D}3}$), 120.3 ($\text{C}^{\text{B}3/\text{D}3}$), 21.7 ($\text{C}^{\text{M}6}$) ppm. IR (solid): $\tilde{\nu} = 3042$ (w), 1684 (w), 1653 (m), 1607 (m), 1578 (w), 1558 (m), 1541 (w), 1506 (w), 1477 (s), 1420 (w), 1315 (w), 1267 (w), 1227 (w), 1165 (w), 1063 (w), 1028 (w), 883 (w), 835 (s), 815 (s), 791 (m), 756 (s), 731 (s), 698 (m), 631 (w) cm $^{-1}$. UV/Vis (CH_2Cl_2 , 1.00×10^{-5} mol dm $^{-3}$): λ_{max} (ϵ) = 228 (43000), 272 (64000), 308 nm (sh, 56000 dm 3 mol $^{-1}$ cm $^{-1}$); emission (CH_2Cl_2 , 1.00×10^{-5} mol dm $^{-3}$, $\lambda_{\text{ex}} = 279$ nm): $\lambda_{\text{em}} = 600$ nm. MS (ESI): $m/z = 823.3$ [$\text{M} - \text{PF}_6$] $^+$ (calcd. 823.2). $\text{C}_{45}\text{H}_{34}\text{F}_6\text{IrN}_4\text{P} \cdot 0.5\text{CH}_2\text{Cl}_2$ (1010.43): calcd. C 54.08, H 3.49, N 5.54; found C 54.00, H 3.53, N 5.66.

[Ir(ppy) $_2$ (2)]PF $_6$], **[Ir(ppy) $_2$ (3)]PF $_6$], and **[Ir(ppy) $_2$ (4)]PF $_6$]: For the preparations, see the Supporting Information.****

[Ir(ppy) $_2$ (2)]PF $_6$]: ^1H NMR (500 MHz, CD_2Cl_2): $\delta = 8.71$ (d, $J = 1.6$ Hz, 1 H, $\text{H}^{\text{F}3}$), 8.69 (d, $J = 8.2$ Hz, 1 H, $\text{H}^{\text{E}3}$), 8.15 (t, $J = 7.9$ Hz, 1 H, $\text{H}^{\text{E}4}$), 7.89 (d, $J = 5.4$ Hz, 1 H, $\text{H}^{\text{E}6}$), 7.85 (m, 3 H, $\text{H}^{\text{B}3+\text{D}3+\text{B}4}$), 7.80 (d $_{\text{AB}}$, $J = 8.6$ Hz, 1 H, $\text{H}^{\text{H}2/\text{H}3}$), 7.76 (overlapping t, $J = 7.9$ Hz, 1 H, $\text{H}^{\text{D}4}$), 7.73 (d $_{\text{AB}}$, $J = 8.6$ Hz, 1 H, $\text{H}^{\text{H}2/\text{H}3}$), 7.70 (d, $J = 5.8$ Hz, 1 H, $\text{H}^{\text{B}6}$), 7.64 (overlapping d, 2 H, $\text{H}^{\text{F}5+\text{D}6}$), 7.54 (d, $J = 7.8$ Hz, 1 H, $\text{H}^{\text{C}3}$), 7.39 (m, 1 H, $\text{H}^{\text{E}5}$), 7.25 (d, $J = 7.8$ Hz, 1 H, $\text{H}^{\text{A}3}$), 7.09 (m, 1 H, $\text{H}^{\text{D}5}$), 7.04 (m, 1 H, $\text{H}^{\text{B}5}$), 6.96 (overlapping m, 2 H, $\text{H}^{\text{C}4+\text{G}4}$), 6.82 (t, $J = 7.5$ Hz, 1 H, $\text{H}^{\text{C}5}$), 6.77 (t, $J =$

7.5 Hz, 2 H, $\text{H}^{\text{G}3}$), 6.61 (t, $J = 7.5$ Hz, overlapping br. signal, 3 H, $\text{H}^{\text{A}4+\text{G}2}$), 6.40 (t, $J = 7.4$ Hz, 1 H, $\text{H}^{\text{A}5}$), 5.97 (d, $J = 7.6$ Hz, 1 H, $\text{H}^{\text{C}6}$), 5.59 (d, $J = 7.6$ Hz, 1 H, $\text{H}^{\text{A}6}$) ppm. ^{13}C NMR (126 MHz, CD_2Cl_2): $\delta = 169.4$ ($\text{C}^{\text{B}2}$), 167.7 ($\text{C}^{\text{D}2}$), 166.6 ($\text{C}^{\text{F}6}$), 158.0 ($\text{C}^{\text{E}2/\text{F}2}$), 157.3 ($\text{C}^{\text{E}2/\text{F}2}$), 151.5 ($\text{C}^{\text{F}4/\text{A}1}$), 150.9 ($\text{C}^{\text{E}6}$), 150.5 ($\text{C}^{\text{F}4/\text{A}1}$), 149.5 ($\text{C}^{\text{B}6/\text{D}6}$), 149.4 ($\text{C}^{\text{B}6/\text{D}6}$), 147.4 ($\text{C}^{\text{C}1}$), 143.5 ($\text{C}^{\text{A}2/\text{C}2}$), 143.2 ($\text{C}^{\text{A}2/\text{C}2}$), 139.9 ($\text{C}^{\text{E}4}$), 138.7 ($\text{C}^{\text{G}1}$), 138.6 ($\text{C}^{\text{B}4/\text{D}4}$), 138.2 ($\text{C}^{\text{B}4/\text{D}4}$), 134.6 ($\text{C}^{\text{H}1}$), 133.4 ($\text{C}^{\text{H}2/\text{H}3}$), 132.0 ($\text{C}^{\text{A}6}$), 131.3 ($\text{C}^{\text{C}5}$), 130.8 ($\text{C}^{\text{C}6}$), 130.2 ($\text{C}^{\text{A}5}$), 129.6 ($\text{C}^{\text{G}4+\text{H}2/\text{H}3}$), 128.4 ($\text{C}^{\text{G}3+\text{E}5}$), 127.9 ($\text{C}^{\text{G}2}$), 127.5 ($\text{C}^{\text{F}5}$), 125.9 ($\text{C}^{\text{E}3}$), 125.1 ($\text{C}^{\text{A}3/\text{C}3}$), 125.0 ($\text{C}^{\text{A}3/\text{C}3}$), 124.0 ($\text{C}^{\text{D}5}$), 123.3 ($\text{C}^{\text{C}4}$), 122.9 ($\text{C}^{\text{B}5}$), 121.4 ($\text{C}^{\text{A}4+\text{F}3}$), 120.4 ($\text{C}^{\text{B}3+\text{D}3}$) ppm: $\text{C}^{\text{H}4}$ signal not observed. IR (solid): $\tilde{\nu} = 3051$ (w), 1684 (w), 1653 (w), 1607 (s), 1583 (m), 1558 (w), 1541 (w), 1522 (w), 1506 (w), 1477 (s), 1439 (w), 1423 (m), 1383 (w), 1315 (w), 1269 (w), 1227 (w), 1163 (m), 1074 (m), 1063 (m), 1030 (m), 1007 (m), 878 (w), 835 (s), 785 (m), 750 (s), 719 (m), 690 (m), 669 (w), 651 (w), 631 (w) cm $^{-1}$. UV/Vis (CH_2Cl_2 , 9.97×10^{-6} mol dm $^{-3}$): λ_{max} (ϵ) = 229 (47000), 271 (66000), 297 nm (sh, 56000 dm 3 mol $^{-1}$ cm $^{-1}$); emission (CH_2Cl_2 , 9.97×10^{-6} mol dm $^{-3}$, $\lambda_{\text{ex}} = 229$ nm): $\lambda_{\text{em}} = 608$, 637 (sh) nm. MS (ESI): $m/z = 887.5$ [$\text{M} - \text{PF}_6$] $^+$ (calcd. 887.2). $\text{C}_{44}\text{H}_{31}\text{BrF}_6\text{IrN}_4\text{P} \cdot 0.6\text{CH}_2\text{Cl}_2$ (1083.79): calcd. C 49.43, H 2.99, N 5.17; found C 49.42, H 2.95, N 5.28.

[Ir(ppy) $_2$ (3)]PF $_6$]: ^1H NMR (500 MHz, CD_2Cl_2): $\delta = 8.65$ (d, $J = 8.2$ Hz, 1 H, $\text{H}^{\text{E}3}$), 8.63 (d, $J = 1.6$ Hz, 1 H, $\text{H}^{\text{F}3}$), 8.16 (t, $J = 7.9$ Hz, 1 H, $\text{H}^{\text{E}4}$), 7.96 (d, $J = 1.5$ Hz, 2 H, $\text{H}^{\text{H}2}$), 7.90 (d, $J = 5.3$ Hz, 1 H, $\text{H}^{\text{E}6}$), 7.89 (t, $J = 1.5$ Hz, 1 H, $\text{H}^{\text{H}4}$), 7.85 (overlapping m, 3 H, $\text{H}^{\text{B}3+\text{D}3+\text{B}4/\text{D}4}$), 7.77 (t, $J = 7.8$ Hz, 1 H, $\text{H}^{\text{B}4/\text{D}4}$), 7.68 (d, $J = 5.8$ Hz, 1 H, $\text{H}^{\text{B}6/\text{D}6}$), 7.63 (d, $J = 5.7$ Hz, 1 H, $\text{H}^{\text{B}6/\text{D}6}$), 7.60 (d, $J = 1.6$ Hz, 1 H, $\text{H}^{\text{F}5}$), 7.55 (d, $J = 7.8$ Hz, 1 H, $\text{H}^{\text{C}3}$), 7.42 (m, 1 H, $\text{H}^{\text{E}5}$), 7.25 (d, $J = 7.8$ Hz, 1 H, $\text{H}^{\text{A}3}$), 7.10 (t, $J = 6.6$ Hz, 1 H, $\text{H}^{\text{B}5/\text{D}5}$), 7.05 (m, 1 H, $\text{H}^{\text{B}5/\text{D}5}$), 6.97 (overlapping t, 2 H, $\text{H}^{\text{C}4+\text{G}4}$), 6.83 (t, $J = 7.5$ Hz, 1 H, $\text{H}^{\text{C}5}$), 6.78 (t, $J = 7.6$ Hz, 2 H, $\text{H}^{\text{G}3}$), 6.62 (t overlapping br. signal, 3 H, $\text{H}^{\text{A}4+\text{G}2}$), 6.40 (t, $J = 7.4$ Hz, 1 H, $\text{H}^{\text{A}5}$), 5.96 (d, $J = 7.6$ Hz, 1 H, $\text{H}^{\text{C}6}$), 5.59 (d, $J = 7.6$ Hz, 1 H, $\text{H}^{\text{A}6}$) ppm. ^{13}C NMR (126 MHz, CD_2Cl_2): $\delta = 169.3$ ($\text{C}^{\text{B}2}$), 167.7 ($\text{C}^{\text{D}2}$), 166.8 ($\text{C}^{\text{F}6}$), 158.0 ($\text{C}^{\text{E}2/\text{F}2}$), 156.8 ($\text{C}^{\text{E}2/\text{F}2}$), 151.1 ($\text{C}^{\text{E}6}$), 150.8 ($\text{C}^{\text{A}1}$), 149.3 ($\text{C}^{\text{B}6/\text{D}6}$), 149.2 ($\text{C}^{\text{B}6/\text{D}6}$), 148.7 ($\text{C}^{\text{F}4}$), 147.1 ($\text{C}^{\text{C}1}$), 143.5 ($\text{C}^{\text{H}1}$), 143.3 ($\text{C}^{\text{A}2+\text{C}2}$), 139.7 ($\text{C}^{\text{E}4}$), 139.4 ($\text{C}^{\text{G}1}$), 138.6 ($\text{C}^{\text{B}4/\text{D}4}$), 138.5 ($\text{C}^{\text{B}4/\text{D}4}$), 136.5 ($\text{C}^{\text{H}4}$), 131.9 ($\text{C}^{\text{A}6}$), 131.3 ($\text{C}^{\text{C}5}$), 130.6 ($\text{C}^{\text{C}6}$), 130.2 ($\text{C}^{\text{A}5}$), 129.7 ($\text{C}^{\text{H}2}$), 129.65 ($\text{C}^{\text{G}4}$), 128.4 ($\text{C}^{\text{E}5}$), 128.3 ($\text{C}^{\text{G}3}$), 127.9 (br., $\text{C}^{\text{G}2}$), 127.7 ($\text{C}^{\text{F}5}$), 125.7 ($\text{C}^{\text{E}3}$), 125.0 ($\text{C}^{\text{A}3}$), 124.9 ($\text{C}^{\text{C}3}$), 124.6 ($\text{C}^{\text{H}3}$), 123.9 ($\text{C}^{\text{B}5/\text{D}5}$), 123.3 ($\text{C}^{\text{C}4}$), 122.9 ($\text{C}^{\text{B}5/\text{D}5}$), 121.3 ($\text{C}^{\text{A}4/\text{F}3}$), 121.2 ($\text{C}^{\text{A}4/\text{F}3}$), 120.3 ($\text{C}^{\text{B}3+\text{D}3}$) ppm. IR (solid): $\tilde{\nu} = 3041$ (w), 1653 (w), 1607 (m), 1582 (w), 1537 (w), 1477 (m), 1442 (w), 1423 (w), 1385 (w), 1356 (w), 1301 (w), 1269 (w), 1225 (w), 1165 (w), 1063 (w), 1030 (w), 878 (w), 831 (s), 785 (m), 754 (w), 727 (m), 702 (m), 694 (w), 651 (w) cm $^{-1}$. UV/Vis (CHCl_3 , 5.04×10^{-6} mol dm $^{-3}$): λ_{max} (ϵ) = 230 (49000), 270 (70000), 395 nm (sh, 6000 dm 3 mol $^{-1}$ cm $^{-1}$); emission (CHCl_3 , 5.15×10^{-5} mol dm $^{-3}$, $\lambda_{\text{ex}} = 232$ nm): $\lambda_{\text{em}} = 635$ nm. MS (ESI): $m/z = 967.30$ [$\text{M} - \text{PF}_6$] $^+$ (calcd. 967.04). $\text{C}_{44}\text{H}_{30}\text{Br}_2\text{F}_6\text{IrN}_4\text{P}$ (1111.72): calcd. C 47.54, H 2.72, N 5.04; found C 47.55, H 2.90, N 5.13.

[Ir(ppy) $_2$ (4)]PF $_6$]: ^1H NMR (500 MHz, CD_2Cl_2): $\delta = 8.77$ (d, $J = 1.5$ Hz, 1 H, $\text{H}^{\text{F}3}$), 8.64 (d, $J = 8.2$ Hz, 1 H, $\text{H}^{\text{E}3}$), 8.15 (m, 1 H, $\text{H}^{\text{E}4}$), 7.97 (overlapping m, 3 H, $\text{H}^{\text{H}2+\text{B}4/\text{D}4}$), 7.92 (d, $J = 5.2$ Hz, 1 H, $\text{H}^{\text{E}6}$), 7.86 (overlapping m, 3 H, $\text{H}^{\text{B}3+\text{D}3+\text{H}4}$), 7.80 (d, $J = 1.5$ Hz, 1 H, $\text{H}^{\text{F}5}$), 7.77 (t, $J = 8.4$ Hz, 1 H, $\text{H}^{\text{B}4/\text{D}4}$), 7.73 (d, $J = 5.8$ Hz, 1 H, $\text{H}^{\text{B}6/\text{D}6}$), 7.65 (overlapping m, 5 H, $\text{H}^{\text{B}6/\text{D}6+\text{I}2}$), 7.56 (d, $J = 7.7$ Hz, 1 H, $\text{H}^{\text{C}3}$), 7.41 (m, 1 H, $\text{H}^{\text{E}5}$), 7.30 (m, 9 H, $\text{H}^{\text{J}3+\text{A}3}$), 7.17 (d, $J = 8.5$ Hz, 4 H, $\text{H}^{\text{I}3}$), 7.14 (d, $J = 7.9$ Hz, 8 H, $\text{H}^{\text{J}2}$), 7.11 (d, $J = 7.3$ Hz, 1 H, $\text{H}^{\text{B}5/\text{D}5}$), 7.07 (overlapping m, 5 H, $\text{H}^{\text{B}5/\text{D}5+\text{J}4}$), 6.98 (overlapping t, 2 H, $\text{H}^{\text{C}4+\text{G}4}$), 6.84 (t, $J = 7.5$ Hz, 1 H, $\text{H}^{\text{C}5}$), 6.78 (t, $J = 7.5$ Hz, 2 H, $\text{H}^{\text{G}3}$), 6.62 (t overlapping broad signal, J

= 7.5 Hz, 3 H, H^{A4+G2}), 6.41 (m, 1 H, H^{A5}), 5.99 (d, $J = 7.6$ Hz, 1 H, H^{C6}), 5.62 (d, $J = 7.6$ Hz, 1 H, H^{A6}) ppm. ¹³C NMR (126 MHz, CD₂Cl₂): $\delta = 169.4$ (C^{B2}), 167.7 (C^{D2}), 166.6 (C^{F6}), 157.8 (C^{E2/F2}), 157.3 (C^{E2/F2}), 151.8 (C^{F4}), 151.4 (C^{A1}), 150.9 (C^{E6}), 149.5 (C^{B6/D6}), 149.3 (C^{B6/D6}), 148.6 (C^{I4}), 148.0 (C^{J1}), 147.4 (C^{C1}), 143.5 (C^{A2/C2/H3}), 143.35 (C^{A2/C2/H3}), 143.3 (C^{A2/C2/H3}), 139.8 (C^{E4}), 138.7 (C^{B4/D4/G1}), 138.6 (C^{B4/D4/G1}), 138.3 (C^{B4/D4/G1}), 136.9 (C^{H1}), 134.1 (C^{I1}), 132.0 (C^{A6}), 131.3 (C^{C6}), 130.8 (C^{C5}), 130.1 (C^{A5}), 129.9 (C^{J3}), 129.6 (C^{G4}), 128.5 (C^{I2}), 128.45 (C^{H4}), 128.4 (C^{E5}), 128.0 (C^{G2/G3/F5}), 127.95 (C^{G2/G3/F5}), 127.9 (C^{G2/G3/F5}), 125.6 (C^{E3}), 125.2 (C^{J2+A4}), 125.0 (C^{C3}), 124.5 (C^{H2}), 124.0 (C^{I3}), 123.9 (C^{B5/D5}), 123.8 (C^{J4}), 123.3 (C^{C4}), 122.9 (C^{B5/D5}), 121.6 (C^{A4/F3}), 121.3 (C^{A4/F3}), 120.45 (C^{B3/D3}), 120.4 (C^{B3/D3}) ppm. IR (solid): $\tilde{\nu} = 3032$ (w), 1684 (w), 1652 (m), 1582 (s), 1555 (m), 1541 (m), 1506 (m), 1477 (m), 1429 (w), 1418 (w), 1387 (w), 1315 (w), 1269 (m), 1225 (w), 1163 (w), 1063 (w), 1030 (w), 876 (w), 833 (s), 785 (w), 752 (m), 727 (m), 692 (s), 669 (w), 660 (w), 648 (w) cm⁻¹. UV/Vis (CHCl₃, 5.00 × 10⁻⁶ mol dm⁻³): λ_{max} (ϵ) = 229 (93000), 256 (92000), 272 (91000), 296 (96000), 342 nm (84000 dm³ mol⁻¹ cm⁻¹); emission (CHCl₃, 5.15 × 10⁻⁶ mol dm⁻³, $\lambda_{\text{ex}} = 229$ nm): $\lambda_{\text{em}} = 604$ nm. MS (ESI): $m/z = 1295.2$ [M - PF₆]⁺ (calcd. 1295.4). C₈₀H₅₈F₆IrN₆P·0.2CH₂Cl₂ (1457.52): calcd. C 66.09, H 4.04, N 5.77; found C 65.95, H 4.05, N 5.94.

CCDC-869670 {for [Ir(ppy)₂(1)]}[PF₆], -869671 {for [Ir(ppy)₂(2)]-[PF₆]} and -869672 {for [Ir(ppy)₂(3)]}[PF₆] contain the supplementary crystallographic data for this paper. These data can be obtained free of charge from The Cambridge Crystallographic Data Centre via www.ccdc.cam.ac.uk/data_request/cif.

Supporting Information (see footnote on the first page of this article): Additional experimental details and crystallographic data.

Acknowledgments

We acknowledge the financial support of the European Union (CELLO, STRP 248043), the Spanish Ministry of Economy and Competitiveness (MINECOM) (MAT2011-24594, CTQ2009-8970), and Consolider-Ingenio on Molecular Nanoscience (CSD2007-00010), and the Generalitat Valenciana (Prometeo/2012/053), the Swiss National Science Foundation, the Swiss National Center of Competence in Research “Nanoscale Science”, the European Research Council (Advanced Grant 267816 LiLo) and the University of Basel. A. P. acknowledges the support of an FPI grant from MINECOM. PD Dr. Daniel Häussinger is thanked for assistance with the low-temperature NMR spectroscopic studies.

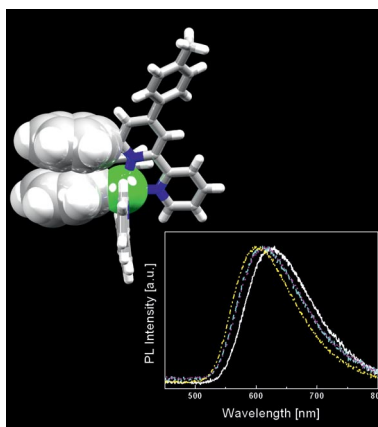
- [1] Q. B. Pei, G. Yu, C. Zhang, Y. Yang, A. J. Heeger, *Science* **1995**, 269, 1086.
- [2] See, for example: J. D. Slinker, A. A. Gorodetsky, M. S. Lowry, J. Wang, S. Parker, R. Rohl, S. Bernhard, G. G. Malliaras, *J. Am. Chem. Soc.* **2004**, 126, 2763.
- [3] R. D. Costa, F. Monti, G. Accorsi, A. Barbieri, H. J. Bolink, E. Ortí, N. Armadori, *Inorg. Chem.* **2011**, 50, 7229, and references cited therein.
- [4] Q. Zhao, S. Liu, M. Shi, C. Wang, M. Yu, L. Li, F. Li, T. Yi, C. Huang, *Inorg. Chem.* **2006**, 45, 6152.
- [5] H. J. Bolink, L. Cappelli, E. Coronado, M. Grätzel, E. Ortí, R. D. Costa, P. M. Viruela, Md. K. Nazeeruddin, *J. Am. Chem. Soc.* **2006**, 128, 14786.
- [6] H.-C. Su, H.-F. Chen, Y.-C. Shen, C.-T. Liao, K.-T. Wong, *J. Mater. Chem.* **2011**, 21, 9653.

- [7] H.-C. Su, H.-F. Chen, F.-C. Fang, C.-C. Liu, C.-C. Wu, K.-T. Wong, Y.-H. Liu, S.-M. Peng, *J. Am. Chem. Soc.* **2008**, 130, 3413, and references cited therein.
- [8] L. He, J. Qiao, L. Duan, G. Dong, D. Zhang, L. Wang, Y. Qiu, *Adv. Funct. Mater.* **2009**, 19, 2950.
- [9] H.-B. Wu, H.-F. Chen, C.-T. Liao, H.-C. Su, K.-T. Wong, *Org. Electron.* **2012**, 13, 483.
- [10] C. Dragonetti, L. Falciola, P. Mussini, S. Righetto, D. Roberto, R. Ugo, A. Valore, F. De Angelis, S. Fantacci, A. Sgamellotti, M. Ramon, M. Muccini, *Inorg. Chem.* **2007**, 46, 8533, and references cited therein.
- [11] M. Lepeltier, T. K.-M. Lee, K. K.-W. Lo, L. Toupet, H. Le Bozec, V. Guerschais, *Eur. J. Inorg. Chem.* **2005**, 110.
- [12] M. S. Lowry, W. R. Hudson, R. A. Pascal, Jr., S. Bernhard, *J. Am. Chem. Soc.* **2004**, 126, 14129.
- [13] G. Kalyuzhny, M. Buda, J. McNeill, P. Barbara, A. J. Bard, *J. Am. Chem. Soc.* **2003**, 125, 6272.
- [14] L. J. Soltzberg, J. D. Slinker, S. Flores-Torres, D. A. Bernards, G. G. Malliaras, H. D. Abruña, J. S. Kim, R. H. Friend, M. D. Kaplan, V. Goldberg, *J. Am. Chem. Soc.* **2006**, 128, 7761.
- [15] H. J. Bolink, E. Coronado, R. D. Costa, E. Ortí, M. Sessolo, S. Graber, K. Doyle, M. Neuburger, C. E. Housecroft, E. C. Constable, *Adv. Mater.* **2008**, 20, 3910.
- [16] R. D. Costa, E. Ortí, H. J. Bolink, S. Graber, C. E. Housecroft, M. Neuburger, S. Schaffner, E. C. Constable, *Chem. Commun.* **2009**, 2029.
- [17] R. D. Costa, E. Ortí, H. J. Bolink, S. Graber, S. Schaffner, M. Neuburger, C. E. Housecroft, E. C. Constable, *Adv. Funct. Mater.* **2009**, 19, 3456.
- [18] R. D. Costa, E. Ortí, H. J. Bolink, S. Graber, C. E. Housecroft, E. C. Constable, *Adv. Funct. Mater.* **2010**, 20, 1511.
- [19] R. D. Costa, E. Ortí, H. J. Bolink, S. Graber, C. E. Housecroft, E. C. Constable, *J. Am. Chem. Soc.* **2010**, 132, 5978.
- [20] R. D. Costa, E. Ortí, H. J. Bolink, S. Graber, C. E. Housecroft, E. C. Constable, *Chem. Commun.* **2011**, 47, 3207.
- [21] F. Neve, A. Crispini, S. Campagna, S. Serroni, *Inorg. Chem.* **1999**, 38, 2250.
- [22] A. J. S. Bexon, J. A. G. Williams, *C. R. Chim.* **2005**, 8, 1326.
- [23] G. W. V. Cave, C. L. Raston, *J. Chem. Soc. Perkin Trans. 1* **2001**, 3258.
- [24] O. Schmelz, M. Rehahn, *e-Polymers* **2002**, 047.
- [25] S. Sprouse, K. A. King, P. J. Spellane, R. J. Watts, *J. Am. Chem. Soc.* **1984**, 106, 6647.
- [26] M. Nonoyama, *Bull. Chem. Soc. Jpn.* **1974**, 47, 767.
- [27] See, for example: R. D. Costa, E. Ortí, D. Tordera, A. Pertegás, H. J. Bolink, S. Graber, C. E. Housecroft, L. Sachno, M. Neuburger, E. C. Constable, *Adv. Energy Mater.* **2011**, 1, 282, and references cited therein.
- [28] I. J. Bruno, J. C. Cole, P. R. Edgington, M. K. Kessler, C. F. Macrae, P. McCabe, J. Pearson, R. Taylor, *Acta Crystallogr., Sect. B* **2002**, 58, 389.
- [29] C. Janiak, *J. Chem. Soc., Dalton Trans.* **2000**, 3885.
- [30] See, for example: E. C. Constable, C. E. Housecroft, E. Schönhofer, J. Schönle, J. A. Zampese, *Polyhedron* **2012**, 35, 154.
- [31] See, for example: M. Mazik, A. C. Buthe, P. G. Jones, *Tetrahedron* **2010**, 66, 385.
- [32] See, for example: J. A. Fernandes, S. M. F. Vilela, P. J. A. Ribeiro-Claro, F. A. Almeida Paz, *Acta Crystallogr., Sect. C* **2011**, 67, o198.
- [33] H. J. Bolink, L. Cappelli, S. Cheylan, E. Coronado, R. D. Costa, N. Lardiés, M. K. Nazeeruddin, E. Ortí, *J. Mater. Chem.* **2007**, 17, 5032.
- [34] D. Tordera, S. Meier, M. Lenes, R. D. Costa, E. Ortí, W. Sarfert, H. J. Bolink, *Adv. Mater.* **2012**, 24, 897.

Received: April 19, 2012
Published Online: ■

LECs: Fine-Tuning Emissions

Four $[\text{Ir}(\text{ppy})_2(\text{N}^{\wedge}\text{N})][\text{PF}_6]$ ($\text{N}^{\wedge}\text{N}$ = 4,6-diphenyl-2,2'-bipyridine derivative) complexes have been synthesized and characterized. In solution, the complexes are short-lived emitters with emission maxima between 600 and 635 nm; the solid-state emission spectra are similar. The performances of the complexes as electroluminescent components in LECs have been evaluated.



A. M. Bünzli, H. J. Bolink,
E. C. Constable,* C. E. Housecroft,*
M. Neuburger, E. Ortí, A. Pertegás,
J. A. Zampese 1–10

Fine-Tuning of Photophysical and Electronic Properties of Materials for Photonic Devices Through Remote Functionalization 

Keywords: Iridium / Ligand design / Photophysical properties / Electroluminescence / X-ray diffraction